ICAST2014 #02

Minimum Energy Cross-Well Actuation of Bistable Piezocomposite Unsymmetric Cross-Ply Plates

Onur Bilgen[1]*, Mehmet R. Simsek[1,2], Andres F. Arrieta[3]

[1] Department of Mechanical and Aerospace Engineering, Old Dominion University, Norfolk, Virginia, 23529, USA
[2] Department of Mechanical Engineering, Turkish Military Academy, 06654, Ankara, Turkey
[3] Laboratory of Composite Materials and Adaptive Structures, ETH Zurich, Zurich, 8092, Switzerland

Abstract

A hybrid unstable-then-stable positive position feedback (PPF) control scheme applied to a bistable unsymmetric cross-ply composite plate with surface-bonded piezoelectric actuators is presented. The plate is clamped on one end for the purpose of forming a low aspect-ratio wing for small UAVs and MAVs. The PPF controller, a simple second-order single-degree-of-freedom system in nature, takes advantage of the first bending mode of the plate about different stable equilibrium positions, and dynamically induces snap-through between the two equilibrium states. Compared to quasi-static actuation, driving the bistable plate dynamically using surface bonded piezoelectric materials requires, theoretically, a lower peak excitation voltage to achieve snap-through. In practice and in most situations, dynamic actuation is the only way to achieve snap-through because of the power density limitation of surface-bonded piezoelectric actuators. The energy consumption to achieve snap-through is automatically minimized by the hybrid feedback control scheme, and undesirable cross-well oscillations are inherently avoided. The proposed control scheme is an improvement over previous strategies where the bistable system was forced at resonance to achieve snap through, where energy consumption is not minimized and chaotic cross-well oscillation may be induced if the actuation amplitude is not precisely determined and controlled. The proposed hybrid PPF controller could be, potentially, applied to any bistable structure where the dynamic stiffness can be minimized on-demand. This is in contrast to permanent mechanical reduction of stiffness techniques where the actuation device loses its passive load carrying capacity for the purpose of increasing its stroke.

1. INTRODUCTION

Bistability is defined as the capability of a structure to adopt two stable states. It has applications in different areas, including control surface design for morphing structures, small UAVs, MAVs, and load alleviation in wind turbine blades, since no energy is required to hold each of the stable states. The bistable property can be achieved in unsymmetric cross-ply composite plates due to residual thermal stresses induced during the curing process (see Hyer [1,2]). The motion from one stable state to another one is physically observed as a jump phenomenon known as snap-through, which is nonlinear in nature (see Arrieta et al. [3]). Nonlinear systems are highly sensitive to their parameters, such as boundary condition, input excitation, initial conditions, etc. As a result, small variation in such parameters can cause a large change in the system response – these can be used to the benefit of the objective at hand. The following sections will briefly summarize a few examples of 1) piezoelectric materials in morphing control surfaces and 2) the use of bistable structures for aerodynamic applications.

1.1. Piezocomposite Control Surfaces

Recently, three review papers have been published on the topic of shape change (morphing) of aircraft by Sofla et al. [4], by Barbarino et al. [5] and by Gomez and Garcia [6]. The publication of these reviews in a two-year period and the continuing developments in materials and electronic systems are indications that morphing in aircraft is becoming more practical and may soon be common in general aviation. An interesting fact is that smooth and continuous aerodynamic control surface designs have been a research interest since the beginning of modern aviation - the first controlled, powered and heavier-than-air flight by the Wright Brothers in 1903. In the context of wing morphing, establishing a wing configuration that is stiff enough to prevent flutter and divergence, but

* Corresponding author, obilgen@odu.edu

compliant enough to allow the range of available motion, has been the central challenge in developing a smooth and continuous wing.

Significant attention in research has been given specifically to using conformal piezoelectric actuators to achieve shape change in variable-camber airfoils. The review article by Barbarino et al. [5] showed that morphing of camber and twist of the wing using piezoelectric materials has resulted in the largest number of wind tunnel and flight tests in aircraft when compared to other morphing categories, such as planform and out-of-plane morphing categories, and also when compared to other actuation sources, such as conventional actuators, shape-memory alloys (SMAs), rubber-muscle actuators and others. In the case of piezoelectric material devices, the rapid development and the reduced cost of small electronics in the last decade has led to several examples of operational small unmanned (and/or remotely piloted) fixed-wing, rotary-wing and ducted-fan aircraft that use smart materials. The following discussion presents a few examples of such aircraft. In 2002, Eggleston et al. [7] experimented with the use of piezoceramic materials, shape-memory alloys, and conventional servomotors in a morphing wing aircraft. A series of wind tunnel tests showed the feasibility of the smart material systems. Barrett et al. [8] employed piezoelectric elements along with elastic elements to magnify the control deflections and forces in aerodynamic surfaces. Vos et al. [9,10] conducted research to improve the Post-Buckled-Precompression concept for aerodynamic applications. Roll control authority was increased on a 1.4 meter span unmanned air vehicle. Kim and Han [11,12] designed and fabricated a flapping wing by using a graphite/epoxy composite material and a Macro-Fiber Composite (MFC) actuator. A twenty percent increase in lift was achieved by changing the camber of the wing at different stages of flapping motion. Bilgen et al. [13,14] presented an application for piezocomposite actuators on a 0.76 meter wingspan morphing wing air vehicle. Adequate roll control authority was demonstrated in the wind tunnel as well as in flight. Bilgen et al. [15,16] presented static flow vectoring via an MFC actuated thin bimorph variable-camber airfoil and an MFC actuated cascading bimorph variable-camber airfoil. Wind tunnel results and analytical evaluation of the airfoils showed comparable effectiveness to conventional actuation systems and no adverse deformation due to aerodynamic loading. Paradies and Ciresa [17] implemented MFCs as actuators into an active composite wing. A scaled prototype wing was manufactured and models were validated with static and preliminary dynamic tests of the prototype wing. Wickramasinghe et al. [18] presented the design and verification of a smart wing for an unmanned aerial vehicle. The proposed smart wing structure consisted of a composite spar and ailerons that have bimorph active ribs consisting of MFC actuators. In 2010, Butt et al. [19,20] and Bilgen et al. [21,22] developed a completely servo-less, wind-tunnel and flight tested remotely piloted aircraft. This vehicle became the first fully solid-state piezoelectric material controlled, non-tethered, flight tested fixed-wing aircraft. Ohanian et al. [23] presented an extensive aerodynamic comparison of a MFC actuated compliant control surface to a servo-actuated conventional control surface for an MAV application. A general methodology for synthesizing the optimal topology of compliant adaptive wings, minimizing the necessary morphing effort, accounting concurrently for 3-D aero-structural interactions, and optimizing the activation levels driving MFC actuators, has been introduced by Molinari et al. [24].

1.2. Bistable Structures

The examples above show the feasibility of piezoelectric materials in small unmanned aircraft; however in most cases in the literature, the actuator works against an elastic component of the system. In order to maintain a static shape, actuation force must be maintained against the elastic restoring force. Considering the fact that piezoelectric material based actuators have some level of resistive (electrical) loss associated with them (regardless of their capacitive nature), maintaining static shape requires work to be done on the system. In this context, bistable structures, mainly bistable composite plates, have been proposed to maintain shape without having to do work on the system. Dano and Hyer [25] demonstrated the actuation of bistable composites using SMA wires and MFC actuators under quasi-static loading. The former showed good actuation authority; however systems incorporating SMAs are difficult to integrate with the bistable composites. Schultz et al. [26] showed that the MFC actuators were simpler to integrate with the bistable structures; however snap-through was achieved in only one direction with the use of static excitation. Furthermore, very high voltages were required to drive the MFC actuator even for very compliant [MFC/0/90/MFC] two-ply plates.

Piezoelectric material actuators would be suitable for morphing structures should they show enough authority to induce and reverse snap-through on bistable composite structures. Such structures must also maintain rigidity in order to be a useful passive load carrying aerodynamic surface. Bistable structures have been applied to aerodynamic applications by several researchers. Mattioni et al. [27, 28, 29] and Diaconu et al. [30, 31] showed the application of bistable composite structures to aerodynamic applications. Daynes et al. [32] used a layered bistable plate structure for a trailing flap demonstrator. Recently, Arrieta et al. [33] and Senba et al. [34] proposed and demonstrated the idea to exploit the rich dynamics of bistable composites to enhance actuation effectiveness. In the

case of Arrieta et al. [33] the morphing strategy was based on the possibility to use external energy from dynamic perturbations on the structure to enhance the authority of an MFC actuator targeting a sub-harmonic resonance of a bistable composite plate, resulting in dynamically triggered snap-through. However, due to symmetric dynamics of the tested plate and lack of authority of the MFC actuator, no reversed snap-through was achieved for the $[0_2/90_2]$ plate. Senba et al. [34] achieved a dynamically triggered reversed snap-through on a $[0/45/MFC^{45}]$ plate of dimensions 148 x 148 mm using an MFC M8557-P1 actuator bonded on the surface with the aid of an added mass approximately equivalent to 100% of that of the tested laminate. It is important to note that the degree of bistability of $[0_n/45_n]$ composites is much smaller than that achieved with a cross-ply $[0_n/90_n]$ lay-up, hence the achievable elastic deformation is greater for the latter type. The added mass increases the effectiveness of dynamic actuation; however the large weight added to the structure is clearly not desirable in morphing structures for aerodynamic applications.

1.3. Previous Research, Objectives and Outline

The brief literature review above shows the merits of exploiting the nonlinear response and dynamic forcing of a bistable composite plate as a morphing strategy. Furthermore, it is well known that for structures which have multiple configurations, such as arches and shells, the load triggering the instability leading to a jump to another stable state is reduced when using dynamic forcing in comparison to static actuation (see Virgin [35]). The key to exploit the nonlinear dynamic response of such structures is the ability to predict important linear dynamic features such as natural frequencies and mode shapes for the available stable states. Some studies of such dynamic characteristics for an unconstrained bistable composite can be found in the literature (see Arrieta et al. [36]; Vogl and Hyer [37]).

As with any active or semi-active compliant aerodynamic surface, a bistable piezocomposite wing is practical if one achieves 1) sufficient aerodynamic load carrying capability in each state and 2) bi-directional snap-through using relatively low excitation voltages, and 3) achieving these functions with minimum energy cost. Such structures can be realized by careful selection of actuator placement, boundary conditions, laminate lay-up, and control scheme. In this context, Arrieta et al. [38, 39, 40] presented the modeling, implementation, and demonstration of purely piezoelectric material induced dynamic forward and reverse snap-through of a bistable unsymmetric composite plate with a clamped edge. Bilgen et al. [41] demonstrated the purely piezoelectric material induced dynamic forward and reverse snap-through of a bistable unsymmetric composite plate with a clamped edge under adverse aerodynamic loading. The objective of the current paper is to demonstrate a similar piezoelectric material induced snap-through in an energy efficient manner and to guarantee a monotonic snap-through without possibility of triggering cross-well oscillations or chaotic response.

The following section briefly presents the resonant control technique that was previously investigated. Next, the design of the bistable composite wing is presented and the results from the wind tunnel experiments on the bistable wing are briefly discussed. Finally, the proposed hybrid unstable-then-stable positive position feedback (PPF) control scheme applied to a bistable unsymmetric cross-ply composite plate with surface-bonded piezoelectric actuators is presented. The paper concludes with a brief discussion of results.

2. RESONANT CONTROL SCHEME

The resonant control technique is very simple in principle. The bistable structure is harmonically excited using the surface bonded piezoelectric materials. By targeting distinct operating frequencies, mainly close to the resonance of each state, the apparent stiffness of the composite plate is dynamically reduced (for that state) which in return enables “forward” snap-through at low peak excitation voltages. This excitation amplitude is lower for dynamic actuation when compared to the quasi-static actuation case. Once the snap-through occurs, the structure maintains its position in that state even if the excitation is still applied. A similar method is followed to go back to the original state. By targeting the resonance of the “second” state, the stiffness is dynamically reduced and “reverse” snap-through is induced. In both cases, once the state changes, the effective bending stiffness is modified and hence the resonance frequency associated with the stable equilibrium is also changed. A carefully selected excitation amplitude, at a distinct frequency, causes resonance in one state and does not cause resonance in the other given that the frequencies are sufficiently separated. This scheme avoids, when the amplitude is selected carefully, undesirable continuous forward and reverse snap-through for a distinct excitation frequency. Complemented with the theoretical modeling, the previous works by the authors have shown that reversible dynamic snap-through can be achieved on bistable composite plates using only surface bonded piezoelectric actuators – even under adverse aerodynamic loading. Inertial augmentation of dynamic excitation has been shown to be the key in transitioning between the two static equilibrium positions; however the excitation amplitude must be selected carefully so that a reverse snap-

through is not induced due to the stored kinetic and potential energy of the system as it crosses the unstable equilibrium.

3. DESIGN OF THE BISTABLE PIEZOCOMPOSITE WING

A partially-active unsymmetrical cross-ply laminate is designed to be bistable by locking-in residual stresses during the elevated-temperature curing process. The composite plate consists of two separate stacking sequences. A large portion of the plate is formed using an unsymmetrical $[0_2/90_2]$ sequence. A much smaller portion is designated as the clamped base and it has a symmetrical $[0/90_2/0]$ sequence. A carbon fiber-epoxy prepreg, type E022-T700 manufactured by SLG [42], is used for each layer. The laminate is cured at elevated temperature. Cooling down to room temperature results in bistable behavior due to the stresses that are locked in due to the elevated temperatures. The rectangular plate is cut in to a tapered planform with a taper ratio of 0.73. The leading-edge (LE) is swept back at an angle of 13.8 deg. A base airfoil structure, which has a NACA 0012 profile, is used to serve as an aerodynamically-shaped clamping mechanism for the base of the bistable plate. The base airfoil adds inertia to the base of the bistable plate so that the boundary, dynamically, behaves similar to a fuselage or a main wing where the bistable wing would be attached to in reality. The complete wing structure has a span of 290 mm, tip chord of 139 mm and root chord of 254 mm. The mean aerodynamic chord is 185 mm.

The Macro-Fiber Composite (MFC) actuator is used to excite the bistable plate. The MFC actuator was originally developed at NASA Langley Research Center [43,44] and offers structural flexibility and high actuation authority. The in-plane poling and subsequent voltage actuation allows the MFC to utilize the *33* piezoelectric effect, which is higher than the *31* effect used by traditional piezoceramic actuators with through-the-thickness poling [45]. Two MFC M8557-P1 type actuators are bonded near the base of the bistable plate on the lower "pressure" surface of the wing. The fibers on the lower surfaces are oriented at 0° which corresponds to the span axis. In order to maximize the out-of-plane bending induced by the MFC actuator, the piezoceramic fibers of the MFC must be close to the effective neutral plane of the unsymmetric cross-ply laminate and the plate must be compliant in bending and stiff in in-plane extension. The analysis of thin MFC actuated structures is presented in Bilgen et al. [46] and the results from that analysis is used to aid the design in the current research. In the case studied here, the out-of-plane deflection induced on the bistable plate by the unidirectional in-plane actuation of the MFC actuator is maximized by bonding the MFC actuator directly on the lower layer with zero degree (spanwise) fiber orientation.

4. OPEN-LOOP RESPONSE OF THE BISTABLE WING

In this section, a preliminary wind-off analysis is conducted to examine the open-loop static and dynamic behavior of the wing while it is mounted on the wind tunnel balance. An MTI Instruments LTC-300-200-SA laser displacement sensor and a Siglab 20-22 analyzer is used to measure the single-point displacement of the complete wing structure mounted in the wind tunnel as shown in Figure 1. In *State 1*, the wing is cambered; however dihedral is nearly zero. There is a very small amount of twist. In *State 2*, the wing has a nearly symmetric profile; however a significant amount of dihedral is clearly visible.

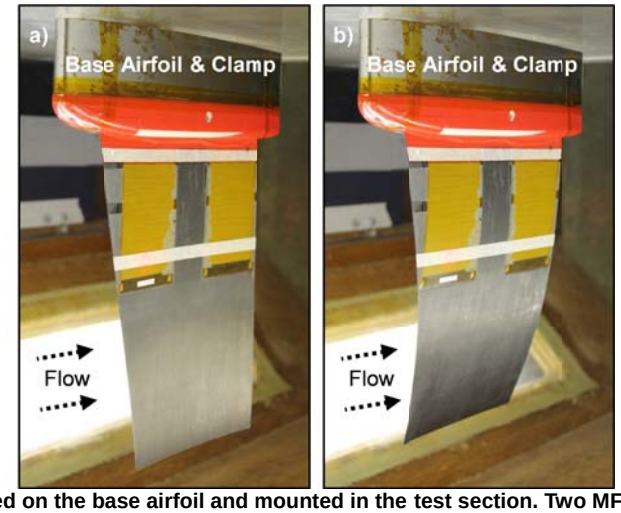

Figure 1: Bistable wing clamped on the base airfoil and mounted in the test section. Two MFC M8557-P1 type actuators are bonded to the lower surface of the bistable wing.

Figure 1a shows the lower surface of the bistable wing in *State 1* which is referred to as the stiff state – its "resonance frequency" about the stable equilibrium position is higher when compared to the other state. Figure 1b

shows the lower surface of the same bistable wing; however in *State 2* which is referred to as the compliant state – its "resonance frequency" about the stable equilibrium point is lower when compared to the other state.

4.1. Dynamic Response

A chirp signal is used for the frequency response function (FRF) measurements, where the excitation is a sine tone with continuously varying frequency in a selected frequency range. The control signal to the MFC actuators is amplified using the TREK 2220 high voltage amplifier. The experiments are conducted at a single excitation voltage level of 200 Vac which is assumed to be in the linear actuation regime. Figure 2 presents the tip-displacement-to-harmonic-excitation FRF comparison of the MFC actuated bistable wing in both states. The experimental results presented in Figure 2 correspond to the different DC offset levels where the DC offset is used to actively change the mean spanwise curvature of the wing and therefore change the effective stiffness about the stable equilibrium positions.

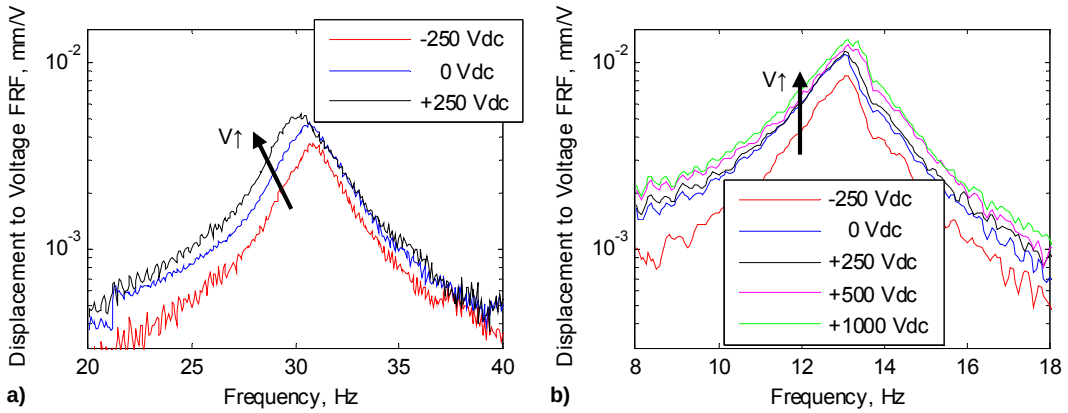

Figure 2: Single-point out-of-plane displacement to harmonic voltage excitation FRF of the bistable piezocomposite wing clamped to the base airfoil and mounted on the wind tunnel load balance. a) *State 1* and b) *State 2*. *Vpeak* = 200 Vac.

Figure 2a presents the frequency response around the first bending resonance of the wing when it is in *State 1* which is designated as the stiff state. The first bending resonance is observed around 30.9 Hz for the bistable plate in *State 1* and excited with a -250 Vdc offset. The resonance frequency for 0 Vdc and +250 Vdc are observed around 30.7 and 30.3 Hz respectively. Note that a DC offset above +500 Vdc causes transition to *State 2* and in fact turns the bistable wing into a monostable wing. This effectively "softening" behavior is expected since the MFC actuators are bonded to the lower surface of the wing. Increasing voltage causes them to induce a bending moment on the structure which moves the structure closer to the unstable equilibrium and hence towards *State 2*.

Similar to above, Figure 2b presents the frequency response around the first bending resonance of the bistable wing when it is in *State 2* which is referred to as the compliant state. The resonance is observed around 13.1 Hz for the wing in *State 1* and excited with a -250 Vdc offset. The resonance frequency for 0 Vdc, +250 Vdc, +500 Vdc and +1000 Vdc are also observed around 13.1 Hz. Note that the curvature induced with the MFC actuators with positive excitation voltages move the wing towards the *State 2* and away from *State 1* stable equilibrium positions. In contrast to the relationship observed for *State 1*, a softening or hardening behavior is not observed as a function of DC offset and hence as a function of curvature. Such behavior, for the range of DC offset values examined here, is expected. Once the wing is in *State 2*, the chordwise curvature distribution along the spanwise direction is roughly zero (see Figure 1). Further change in the spanwise curvature, induced by the MFC actuators, do not strongly couple into the chordwise curvature distribution; therefore the spanwise bending stiffness of the wing remains relatively fixed. Since the energy density of the MFC actuator is relatively limited, the observation above remains valid for the DC offset values that are attainable by the actuator.

The FRF tests that are presented above indicate the resonance frequencies for both states where a large amount of deformation can be achieved with the low excitation voltage. The tests also suggest that the DC offset values can be used to fine tune the dynamic behavior of the bistable wing. A set of discrete trials are conducted to see if snap-through can be achieved dynamically in the wind-off condition. Note that the MFC actuator has a recommended voltage range of -500 to +1500 Volts. Excitation voltages below -800 Vdc typically re-polarize the PZT fibers. On the other hand, excitation voltages above +1800 Vdc typically result in shortages in the form of dielectric breakdown of the PZT material and/or the epoxy matrix. The combination of the AC (amplitude) and the DC (offset) excitation values are selected so that these over-range limits are not exceeded.

Table 1: Wind-off dynamic snap-through behavior of the bistable wing from two different stable equilibriums.

State	DC Offset, Vdc	Excitation Frequency, Hz	Is Snap Achieved for [Vac values] ?
1 to 2	-250	30.8	No: [≤500]
	0	30.6	No: [≤600]
	+250	29.9	Yes: [≈800]
	+500	n/a	Yes: [with small disturbance]
2 to 1	-250	13.1	No: [≤500]
	0	13.1	Yes: [≈700]
	+250	13.1	No: [≤1000]
	+500	13.1	No: [≤1000]
	+1000	13.1	No: [≤700]

In Table 1, it is observed that snap-through from *State 1* to *State 2* can be achieved with a sinusoidal excitation with 800 Vac amplitude at 29.9 Hz and with +250 Vdc offset. Higher excitation amplitudes will also result in snap-through. Snap-through from *State 2* to *State 1* can be achieved with a sinusoidal excitation with 700 Vac amplitude at 13.1 Hz and with 0 Vdc offset. These initial observations in the wind-off condition will be used as a guide to determine the excitation parameters during the wind-on experiments which will be presented in the next section.

4.2. Static Response

The static response is also examined to determine if snap-through can be achieved. A test is conducted where the DC excitation is started from -700 Volts, in *State 1*, and increased to +1700 Volts. During the increasing portion of the test, a snap-through is observed in the +500 to +1000 V range in different trials. The variation of the snap-through voltage is due to the past-history of the excitation (e.g. stresses stored in the memory of the structure due to hysteresis). Once a snap-through occurs from *State 1* to *State 2*, the structure is no longer bistable due to the static curvature induced by the MFC actuator. The test procedure is continued where the excitation is decreased from +1700 to -700 Volts. The specimen does become bistable as voltage is reduced; however snap-through is not achievable, with static excitation, from *State 2* to *State 1*. Table 2 presents the static snap-through behavior in detail.

Table 2: Wind-off static snap-through behavior of the bistable wing from two different stable equilibriums.

DC Offset, Vdc	Bistable ?	Snap from 1 to 2 for increasing Vdc ?	Snap from 2 to 1 for decreasing Vdc ?
-700	Yes	No	No
-500	Yes	No	No
-250	Yes	No	No
0	Yes	No	No
+250	Yes	No	No
+500	Transition	Yes (with small disturbance)	No
+1000	Transition	Yes (with small disturbance)	No
+1250	No	Yes	No
+1500	No	Yes	No
+1700	No	Yes	No

From the data given in Table 1 and Table 2, it appears that the static excitation can achieve snap-through from *State 1* to *State 2* at a lower peak excitation value when compared to the dynamic excitation. This observation is artificially caused by the wind tunnel and the load-balance setup. The complete wing structure which consists of the bistable wing and the base airfoil is connected to the load balance with a sting. The sting, from the load balance to the root of the base airfoil is 419 mm long; therefore the boundary condition effective to the base airfoil and the bistable wing in the wind tunnel is a combination of a translational spring and a torsional spring. A dynamic excitation using the MFC actuator results in lower curvatures in the bistable-wing because of the compliance in the boundary condition in the wind tunnel.

5. RESPONSE TO RESONANT CONTROL IN THE WIND TUNNEL

This section presents the aerodynamic behavior of the bistable piezocomposite wing in the wind tunnel. The experiments were conducted in a low speed, open circuit and closed test section wind tunnel facility. Two types of tests were conducted. (1) The first type of test is to understand the natural (passively induced) snap-through that is caused by an “adverse” pressure gradient induced on the structure as a result of freestream. The objective is to demonstrate the fact that the structure can sustain a certain level of adverse pressure gradient without snapping to another state. This property, if demonstrated, shows the passive load carrying capability. The critical values of snap-inducing velocity and AOA are key values in determining the passive load carrying capability. (2) The second test is conducted to understand the actively induced snap-through that is caused due to the strain induced by the MFC actuator. The objective is to demonstrate that the structure can be made, effectively, monostable against a certain

level of adverse pressure gradient. This property, if demonstrated, shows the controllability of a desired state. The critical values of voltage excitation amplitude, frequency (and DC offset if necessary) are key values in determining the controllability property.

For both types of tests, a set of AOA sweeps are conducted in the range of 10 to 20 m/s nominal velocity values – the velocity range is swept in 2.5 m/s steps. The AOA sweep is conducted, in both directions, in the range of -20 to +20°. The AOA range is swept in 0.5° steps. The main purpose for varying the freestream velocity and the AOA is to simulate the working environment for such a structure. More precisely, the distribution of the pressure is simulated mainly by varying the AOA and the net pressure acting on the wing is mainly simulated by varying the freestream velocity. An important detail to note is that all of the wind tunnel tests on the bistable wing are conducted without removing the specimen and without changing its mounting angle with respect to the rotary table. This consistency between different tests allows for a fair comparison and allows certain conclusions to be made regarding the load carrying capability and the snap-through behavior.

5.1. Snap-Through from State 2 to State 1

First, the excitation parameters that induce snap-through from *State 2* to *State 1* are identified from previous wind-off experiments. A sinusoidal excitation with 800 Vac amplitude at 13.0 Hz is applied which corresponds to the resonance frequency of *State 2*. This excitation causes the wing to be effectively monostable for *State 1*. Next, a fixed freestream velocity is selected and applied. The AOA is started at -20° where both the dynamic excitation and the pressure gradient is favorable to *State 1*. In addition, further increase in the magnitude (e.g. AOA < -20°) does not induce snap-through to *State 2*. The AOA is incremented in 0.5° steps. As the AOA is increased, the favorable pressure gradient to *State 1* switches, at an unknown value, to the adverse pressure gradient to *State 1*. The pressure gradient becomes favorable to the *State 2*. Further increase in the AOA may cause the adverse pressure gradient to induce snap-through from *State 1* to *State 2* at a critical AOA value; however this critical AOA value is reduced by the "disturbance" of the sinusoidal excitation when compared to the passive wing. The cycle is reversed when starting the AOA at +20° and reducing it to -20°. The snap-through from *State 2* to *State 1* will occur at a critical AOA value regardless of the net pressure because of the dynamic excitation. A critical freestream velocity still exists for a preselected range of AOA; however this critical velocity value is lower than the one observed for the passive structure. Below the critical freestream velocity, *State 1* can be held for the entire AOA range that is of interest even in the presence of dynamic excitation tuned for the resonance of *State 2*. Figure 3 presents the lift coefficient response of the bistable plate at three different freestream velocities where the AOA is first swept up from -20° to +20° and swept back down to -20°. The path *abcdefa* is indicated in the figures to aid the discussion. The wing is set at *State 1* which is the favorable state at -20° AOA. Figure 3a presents the passive behavior and Figure 3b presents the behavior with the excitation. Figure 3 also presents the theoretical finite-wing lift curve for reference. The independent variable is the pitch angle of the base airfoil. The AOA up and down sweeps are averaged for certain tests due to lack of aerodynamic hysteresis and snap-through.

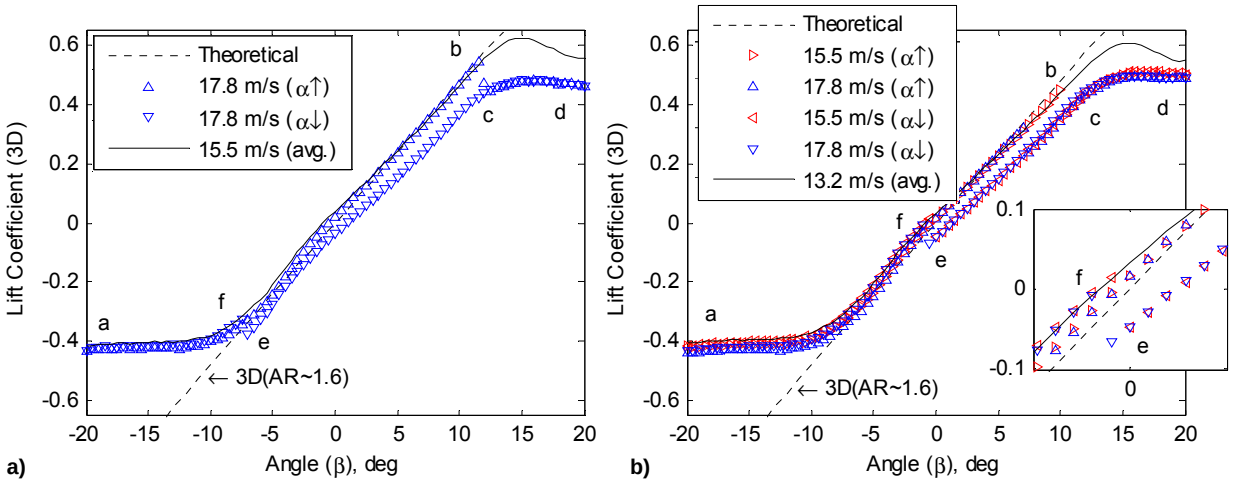

Figure 3: Experimental (3D) lift coefficient of the bistable wing to rotation angle sweep (up-down) and free-stream velocity. a) Passive, b) Sine tone excitation at 13.0 Hz, 800 Vac amplitude and 0 Vdc offset. Re_{MAC} = 162,000, 189,000 and 218,000.

For the passive wing, a snap-through is not observed for the complete AOA range, in both directions, at 15.5 m/s and all other velocities below this value. In contrast, at 17.8 m/s, snap-through is observed in both directions as expected – indicating that the critical velocity value is in the range of 15.5 to 17.8 m/s. Similarly, for the active

wing, a snap-through is not observed for the complete AOA range, in both directions, at 13.2 m/s and all other velocities below this velocity value. In contrast, at 15.5 and 17.8 m/s, snap-through is observed in both direction as expected – indicating that the critical velocity value is in the range of 13.2 to 15.5 m/s. (Note: If a gust causes the wing to go in to *State 2*, snap-through from *State 2* to *State 1* is always guaranteed for velocities below the critical velocity independent of the AOA.) In contrast to the passive structure, a dynamically induced snap-through from *State 2* to 1 is observed near zero degree of the mount angle where the pressure gradient is near neutral (see the path *ef* in Figure 3b). The snap-through occurs at -0.5° and 0.0° for the velocities of 17.8 and 15.5 m/s respectively indicating that the dynamic excitation can achieve snap-through from *State 2* to *State 1* by tailoring the composite and optimizing the distribution of actuation.

5.2. Snap-Through from State 1 to State 2

Similar to the discussion above, Figure 4 presents the lift coefficient response of the passive and active bistable plate at three different freestream velocities where the AOA is first swept down from +20° to -20° and swept back up to +20°. The wing is set at *State 2* which is the favorable state at +20° AOA due to pressure gradient and also favorable due to dynamic excitation at the resonance frequency of *State 1*. For the active case, a sinusoidal excitation with 1000 Vac amplitude at 30.0 Hz and 300 Vdc offset is applied - the excitation frequency is near the resonance frequency of *State 1*.

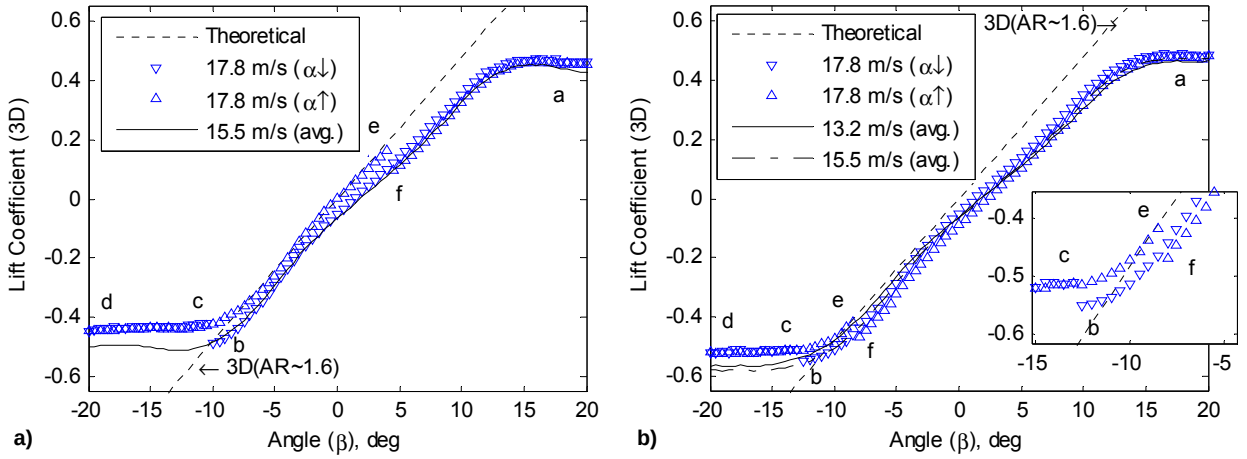

Figure 4: Experimental (3D) lift coefficient of the bistable wing to rotation angle sweep (down-up) and free-stream velocity. a) Passive, b) Sine tone excitation at 30.0 Hz, 1000 Vac amplitude and 300 Vdc offset. Re_{MAC} = 162,000, 189,000 and 218,000.

For the passive wing, the response for the AOA down-up sweep is very similar to the previously presented AOA up-down sweep. A snap-through is not observed for the complete AOA range, in both directions, at 15.5 m/s and all other velocities below this value. In contrast, at 17.8 m/s, snap-through is observed in both directions as expected – indicating that the critical velocity value is in the range of 15.5 to 17.8 m/s. For the active wing, a snap-through is not observed for the complete AOA range, in both directions, at 13.2 and 15.5 m/s and all other velocities below the value of 13.2 m/s. In contrast, at 17.8 m/s, snap-through is observed in both directions – indicating that the critical velocity value is in the range of 15.5 to 17.8 m/s. In the case where *State 2* is the desired state, the dynamic excitation is clearly capable of achieving *State 2* in the presence of adverse pressure gradient (see the path *ef* in Figure 4b) before it is triggered aerodynamically.

6. MINIMUM ENERGY POSITIVE POSITION FEEDBACK CONTROL SCHEME

The PPF controller, originally proposed by Goh [47] and developed by Goh and Caughey [48] as an alternative to collocated direct velocity feedback, has the following advantages: 1) the stability condition is non-dynamic; 2) it is not sensitive to spillover; 3) it is not destabilized by finite actuator dynamics; 4) it is amenable to a strain-based sensing approach, which are experimentally validated by Fanson and Caughey [49]. In addition, it offers quick damping for a particular mode if the modal characteristics are well known. PPF controllers have been extensively used in flexible structure vibration control applications, such as in a programming structure by Dosch et al. [50], a thermally induced vibration by Friswell et al. [51], a slewing flexible frame by Leo and Inman [52], and a thin film rigidizable inflatable boom by Tarazaga et al. [53]. As illustrated in Figure 5, the PPF control algorithm introduces a second-order filter (G1) to the system (H), which is fed by the sensed position signal. The position response of the filter is then fed back to give the force input to the structure.

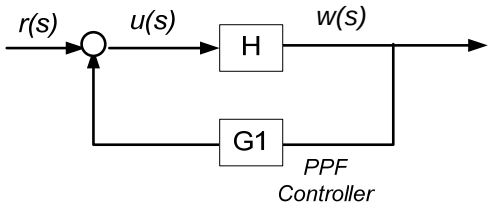

Figure 5: Block diagram of the PPF controller.

In the figure, r is the reference signal, u corresponds to the voltage output to the piezoceramic and w is the tip displacement of the wing. The structure and the PPF controller equations for the scalar case are:

$$\ddot{w} + 2\zeta\omega_n \dot{w} + {\omega_n}^2 w = b\,u \tag{1}$$

$$\ddot{u} + 2\zeta_f\omega_f \dot{u} + {\omega_f}^2 u = g_f\,{\omega_f}^2\,w \tag{2}$$

where ζ and ω_n indicate the damping ratio and natural frequency respectively, and b is the input gain. The actual value of input gain b is not constant as the voltage/strain level changes, which is confirmed in Bilgen et al. [54] and also discussed by Crawley and Anderson [55]. In this section, an average b value is found experimentally. The controller parameters ζ_f *and* ω_f correspond to damping ratio and natural frequency respectively. The control gain is denoted as g_f and it is simply a linear amplification of the feedback signal. Saturation is introduced in the control diagram so that the voltage limits of the MFCs are not exceeded. The transfer functions of the structure and controller in Laplace form are given by:

$$H(s) = \frac{b}{s^2 + 2\xi\omega_n\, s + {\omega_n}^2} \tag{3}$$

$$G1(s) = \frac{g_f\,{\omega_f}^2}{s^2 + 2\xi_f\omega_f\, s + {\omega_f}^2} \tag{4}$$

The two second-order systems are forming a simple two-DOF system. The PPF controller, in its conventional (stable) setup acts as a simple "mechanical" vibration absorber. In this paper, the hybrid unstable-then-stable PPF controller is proposed to dynamically reduce the stiffness of the bistable structure. In the unstable state, where the feedback multiplier is "-1", the dynamic stiffness is minimized causing a typical resonant behavior with increasing amplitude. As soon as the desired displacement is reached, the unstable equilibrium in this case, the feedback multiplier is set to "+1" causing the controller to be stable. Table 2 indicates the parameters for the wing at each state and the corresponding PPF controllers. From Eq. 2 and Table 3, it is observed that the PPF controller has the same form as the system represented by Eq. 1, but with a higher damping ratio.

Table 3: Parameters for the bistable wing and the hybrid PPF controller.

	Operating Frequency	Damping Ratio	Gain
Wing - State 1	$\omega_n = 191.6$ rad/s	$\zeta = 0.038$	$b = 266.1$ (mm/s^2)/V
Wing - State 2	$\omega_n = 81.05$ rad/s	$\zeta = 0.036$	$b = 198.7$ (mm/s^2)/V
PPF Controller - State 1	$\omega_f = 219.9$ rad/s	$\zeta_f = 0.50$	$g_f = 0.500$ V/mm
PPF Controller - State 2	$\omega_f = 94.25$ rad/s	$\zeta_f = 0.30$	$g_f = 0.0700$ V/mm

The PPF controller is programmed using Simulink, a toolbox in MATLAB software. A simple code written in dSPACE Control Desk software is used to implement the controller on a dSPACE 1104 real time control board. The tip displacement of the wing is measured with an MTI Instruments LTC-300-200-SA type laser displacement sensor. The output of the controller is fed to the MFC actuator using a TREK 2220 high voltage amplifier with 200x gain. First, a set of conventional control analyses are conducted on the passive bistable wing to understand the change in the dynamic behavior under control gains. Next, by the use of the hybrid feedback control technique, the plate is turned into an effectively monostable structure, or alternatively, both stable equilibrium positions can be reached actively from the other stable equilibrium with minimum control effort. Dynamic and monotonic forward (Figure 6) and reverse (Figure 7) snap-through is demonstrated in in bench top experiments which show the effectiveness of the proposed hybrid feedback control scheme through piezoelectric actuation. In the figures, w_{s10} and w_{s20} indicate

the stable equilibrium positions of *State 1* and *State 2* respectively. The label w_{u0} indicates the unstable equilibrium position.

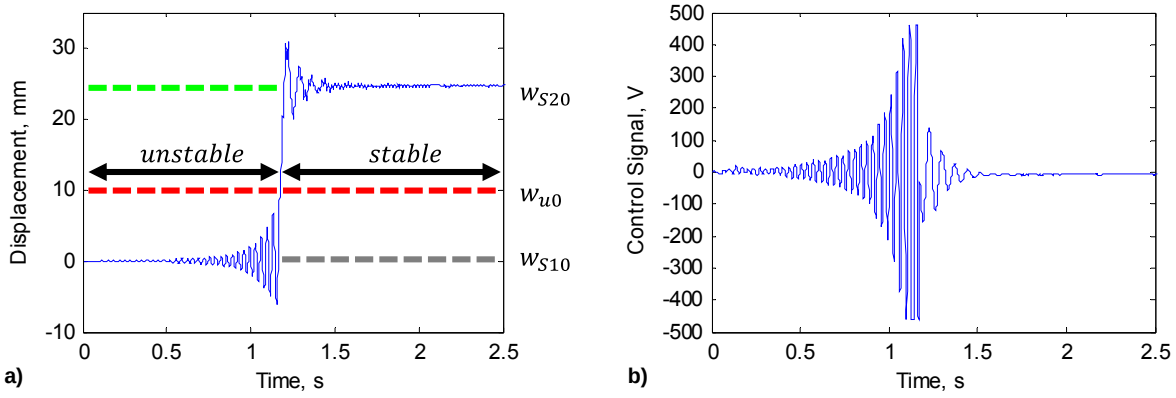

Figure 6: Transition from State 1 to State 2 using the hybrid PPF controller. a) Response, b) control effort.

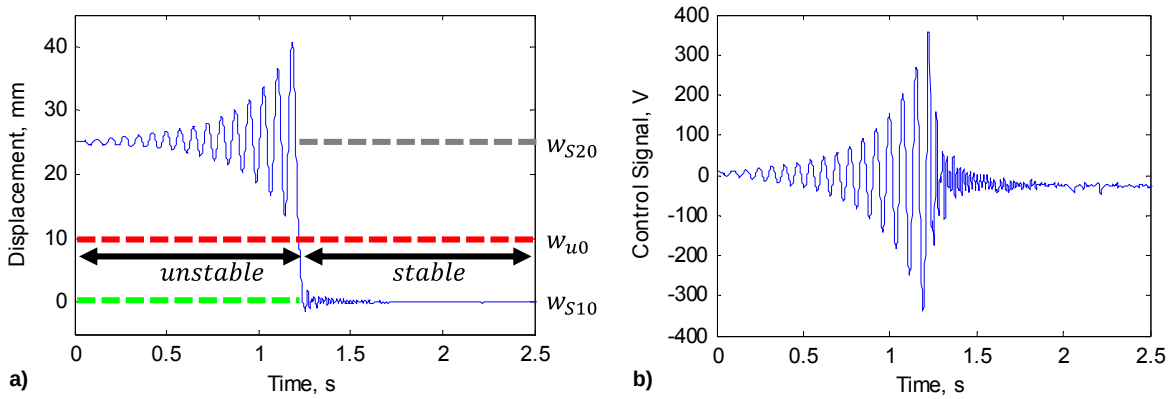

Figure 7: Transition from State 2 to State 1 using the hybrid PPF controller. a) Response, b) control effort.

7. CONCLUSIONS

A hybrid unstable-then-stable PPF control scheme applied to a bistable unsymmetric cross-ply composite plate with surface-bonded piezoelectric actuators is successfully demonstrated. The energy consumption to achieve snap-through is automatically minimized by the hybrid feedback control scheme, and undesirable cross-well oscillations are inherently avoided. The modified PPF controller could be, potentially, applied to any bistable stiffness where the stiffness can be minimized on-demand. This is in contrast to permanent mechanical reduction of stiffness techniques where the actuation device loses its passive load carrying capacity for the purpose of increasing its stroke.

ACKNOWLEDGMENTS

The financial and equipment support from the Old Dominion University Equipment Trust Fund and the Frank Batten College of Engineering and Technology are acknowledged. Mehmet R. Simsek would like to thank to Turkish Land Forces and Turkish Military Academy for their financial and all other support. This work was partially supported by the European Research Council grant number 247045 entitled "Optimisation of Multi-scale Structures with Applications to Morphing Aircraft". The authors would like to thank Professor Helmut Schürmann and Mr. Hasan Dadak of the Fachgebiet Konstruktiver Leichtbau und Bauweisen (KLuB) group at the Technische Universität Darmstadt for their support in the manufacturing of the tested composite specimens.

REFERENCES

[1] Hyer, M. W., "Some observations on the cured shapes of thin unsymmetric laminates," *Journal of Composite Materials*, Vol. 15, 1981, pp. 175–194.
[2] Hyer, M. W., "Calculations of the room-temperature shapes of unsymmetric laminates," *Journal of Composite Materials*, Vol. 15, 1981, pp. 296–310.

[3] Arrieta, A. F., Neild, S. A. and Wagg, D. J., "On the cross-well dynamics of a bi-stable composite plate," *Journal of Sound and Vibration*, Vol. 330, 2010, pp. 3424-3441.
[4] Sofla, A. Y. N., Meguid, S. A., Tan, K. T. and Yeo, W. K., "Shape morphing of aircraft wing: Status and challenges," *Materials and Design*, Vol. 31, 2010, pp. 1284-1292. doi:10.1016/j.matdes.2009.09.011
[5] Barbarino, S., Bilgen, O., Ajaj, R. M., Friswell, M. I. and Inman, D. J., "A Review of Morphing Aircraft," *Journal of Intelligent Material Systems and Structures*, Vol. 22, No. 9, 2011, pp. 823-877. doi: 10.1177/1045389X11414084
[6] Gomez, J. C. and Garcia, E., "Morphing unmanned aerial vehicles," *Smart Materials and Structures*, Vol. 20, 103001, 2011, 16pp. doi:10.1088/0964-1726/20/10/103001
[7] Eggleston, G., Hutchison, C., Johnston, C., Koch, B., Wargo, G. and Williams, K., "Morphing Aircraft Design Team," Virginia Tech Aerospace Engineering Senior Design Project, 2002.
[8] Barrett, R. M., Vos, R., Tiso, P. and De Breuker, R., "Post-Buckled Precompressed (PBP) Actuators: Enhancing VTOL Autonomous High Speed MAVs," 46th AIAA/ASME/ASCE/AHS/ASC Structure, Structural Dynamics & Materials Conference, AIAA 2005-2113, Austin, TX, 2005.
[9] Vos, R., De Breuker, R., Barrett, R. and Tiso, P., "Morphing Wing Flight Control via Postbuckled Precompressed Piezoelectric Actuators," *Journal of Aircraft*, Vol. 44, No. 4, 2007.
[10] Vos, R., Barrett, R. and Zehr, D., "Magnification of Work Output in PBP Class Actuators Using Buckling/Converse Buckling Techniques," 49th AIAA/ASME/ASCE/AHS/ASC Structures, Structural Dynamics, and Materials Conference, Schaumburg, IL, AIAA 2008-1705, 2008.
[11] Kim, D. K. and Han, J. H., "Smart Flapping Wing using Macro-Fiber Composite Actuators," Proceedings of SPIE Vol. 6173, 61730F, 2006, pp. 1-9.
[12] Kim, D. K., Han, J. H. and Kwon, K. J., "Wind Tunnel Tests for a Flapping Wing Model with a Changeable Camber using Macro-Fiber Composite Actuators," *Smart Materials and Structures*, Vol. 18, No. 2, 2009.
[13] Bilgen, O., Kochersberger, K. B., Diggs, E. C., Kurdila, A. J. and Inman, D. J., "Morphing Wing Micro-Air-Vehicles via Macro-Fiber-Composite Actuators," 48th AIAA/ASME/ASCE/AHS/ASC Structures, Structural Dynamics, and Materials Conference, Honolulu, HI, AIAA-2007-1785, 2007.
[14] Bilgen, O., Kochersberger, K. B. and Inman, D. J., "Macro-Fiber Composite Actuators for a Swept Wing Unmanned Aircraft," *Aeronautical Journal*, Special issue on Flight Structures Fundamental Research in the USA, publication of Royal Aeronautical Society, Vol. 113, No. 1144, 2009.
[15] Bilgen, O., Kochersberger, K. B., Inman, D. J. and Ohanian, O. J., "Macro-Fiber Composite Actuated Simply-Supported Thin Morphing Airfoils," *Smart Materials and Structures*, Vol. 19, 055010, 2010. doi:10.1088/0964-1726/19/5/055010
[16] Bilgen, O., Kochersberger, K. B., Inman, D. J. and Ohanian, O. J., "Novel, Bi-Directional, Variable Camber Airfoil via Macro-Fiber Composite Actuators," *Journal of Aircraft*, Vol. 47, No. 1, 2010, pp. 303-314. doi: 10.2514/1.45452
[17] Paradies, R. and Ciresa, P., "Active wing design with integrated flight control using piezoelectric macro fiber composites," *Smart Materials and Structures*, Vol. 18, 2009. doi:10.1088/0964-1726/18/3/035010
[18] Wickramasinghe, V. K., Chen, Y., Martinez, M., Kernaghan, R. and Wong, F., "Design and Verification of a Smart Wing for an Extremely-Agile Micro-Air-Vehicle,", 50th AIAA/ASME/ASCE/AHS/ASC Structures, Structural Dynamics, and Materials Conference, Palm Springs, CA, AIAA 2009-2132, 2009.
[19] Butt, L., Day, S., Sossi, C., Weaver, J., Wolek, A., Bilgen, O., Inman, D.J. and Mason, W.H., "Wing Morphing Design Team Final Report 2010," Virginia Tech Departments of Mechanical Engineering and Aerospace and Ocean Engineering Senior Design Project, Blacksburg, VA, 2010.
[20] Butt, L., Bilgen, O., Day, S., Sossi, C., Weaver, J., Wolek, A., Inman, D.J. and Mason, W.H., "Wing Morphing Design Utilizing Macro Fiber Composite," Society of Allied Weight Engineers (SAWE) 69th Annual Conference, Virginia Beach, VA, Paper Number 3515-S, 2010.
[21] Bilgen, O., Butt, L.M., Day, S.R., Sossi, C.A., Weaver, J.P., Wolek, A., Mason, W.H. and Inman, D.J., "A Novel Unmanned Aircraft with Solid-State Control Surfaces: Analysis and Flight Demonstration," 52nd AIAA/ASME/ASCE/AHS/ASC Structures, Structural Dynamics, and Materials, Denver, CO, 2011.
[22] Bilgen, O., Butt, L.M., Day, S.R., Sossi, C.A., Weaver, J.P., Wolek, A., Mason, W.H. and Inman, D.J., "A Novel Unmanned Aircraft with Solid-State Control Surfaces: Analysis and Flight Demonstration," *Journal of Intelligent Material Systems and Structures*, Vol. 24, No. 2, 2012, pp. 147–167. doi: 10.1177/1045389X12459592
[23] Ohanian, O. J., Hickling, C., Stiltner, B., Karni, E. D., Kochersberger, K. B., Probst, T., Gelhausen, P. A. and Blain, A. P., "Piezoelectric Morphing versus Servo-Actuated MAV Control Surfaces," 53rd AIAA/ASME/ASCE/AHS/ASC Structures, Structural Dynamics and Materials Conference, Honolulu, HI, AIAA 2012-1512, 2012.
[24] Molinari, G., Arrieta, A. F. and Ermanni, P., 2014, "Aero-Structural Optimization of Three-Dimensional Adaptive Wings with Embedded Smart Actuators", *AIAA Journal*, Vol. 52, No. 9, pp. 1940-1951. doi: 10.2514/1.J052715
[25] Dano, M. L. and Hyer, M. W., "Sma-induced snap-through of unsymmetric fiberreinforced composite laminates," *International Journal of Solids and Structures*, Vol. 40, 2003, pp. 5949–5972.
[26] Schultz, M. R., Hyer, M. W., Williams, R. B., Wilkie, W. K. and Inman, D. J., "Snap-through of unsymmetric laminates using piezocomposite actuators," *Composites Science and Technology*, Vol. 66, 2006, pp. 2442–2448.
[27] Mattioni, F., Weaver, P. M. and Friswell, M. I., "The Application of Multi-stable Composites to Morphing Structures," International Conference on Adaptive Structures and Technologies (ICAST), Paris, France, 2005, pp. 45-52.

[28] Mattioni, F., Weaver, P. M., Potter, K. D. and Friswell, M. I., "The application of thermally induced multistable composites to morphing aircraft structures," SPIE Smart Structures and Materials & Nondestructive Evaluation and Health Monitoring, 2008, pp. 6930-6938.
[29] Mattioni, F., "Thermally induced multi-stable composites for morphing aircraft applications," Ph.D. Dissertation, University of Bristol, Bristol, United Kingdom, 2009.
[30] Diaconu, C. G., Weaver, P. M. and Mattioni, F., "Concepts for morphing airfoil sections using bistable laminated composite structures," *Thin-Walled Structures*, Vol. 46, No. 6, 2008, pp. 689-701. ISSN: 0263-8231, doi: 10.1016/j.tws.2007.11.002
[31] Diaconu, C. G., Weaver, P. M. and Arrieta, A. F., "Dynamic analysis of bistable composite plates," *Journal of Sound and Vibration*, Vol. 22, 2009, pp. 987–1004.
[32] Daynes, S., Weaver, P. M. and Potter, K. D., "Aeroelastic study of bistable composite airfoils," *Journal of Aircraft*, Vol. 46, No. 6, 2009, pp. 2169-2173. doi: 10.2514/1.44287.
[33] Arrieta, A. F., Wagg, D. J. and Neild, S. A., "Dynamic snap-through for morphing of bi-stable composite plates," *Journal of Intelligent Material Systems and Structures*, Vol. 22, 2011, pp. 103-122.
[34] Senba, A., Ikeda, T. and Ueda, T., "A two-way morphing actuation of bistable composites with piezoelectric fibers," 51st AIAA/ASME/ASCE/AHS/ASC Structures, Structural Dynamics and Materials Conference, 2010.
[35] Virgin, L. N., *Vibration of Axially-Loaded Structures*, Cambridge University Press, Cambridge, 2007.
[36] Arrieta, A. F., Spelsberg-Korspeter, G., Neild, S. A., Hagedorn, P. and Wagg, D. J., "Low order model for the dynamics of a bistable composite plate," *Journal of Intelligent Material Systems and Structures*, 2011. doi: 10.1177/1045389X11422104
[37] Vogl, G. A. and Hyer, M. W., "Natural vibration of unsymmetric cross-ply laminates," *Journal of Sound and Vibration*, 2011.
[38] Arrieta, A. F., Bilgen, O., Friswell, M. I. and Hagedorn, P., "Dynamic control for morphing of bi-stable composites,' special issue in *Journal of Intelligent Material Systems and Structures*, in press, published online, 2012. doi: 10.1177/1045389X12449918
[39] Arrieta, A. F., Bilgen, O., Friswell, M. I. and Hagedorn, P., "Passive load alleviation bi-stable morphing concept," *AIP Advances*, Vol. 2, 032118, 2012. doi: 10.1063/1.4739412
[40] Arrieta, A. F. Bilgen, O., Friswell, M. I., and Ermanni, P., 2013, "Modelling and configuration control of wing-shaped bi-stable piezoelectric composites under aerodynamic loads," Aerospace Science and Technology, Vol. 29, pp. 453-461. doi: 10.1016/j.ast.2013.05.004
[41] Bilgen, O., Arrieta, A. F., Friswell, M. I. and Hagedorn, P., 2013, "Dynamic Control of a Bistable Wing under Aerodynamic Loading,' Smart Materials and Structures, Vol. 22, 025020. doi:10.1088/0964-1726/22/2/025020
[42] SLG, High-Performance Prepregs: Preimpregnated Products for Fiber-Reinforced Composites, SLG Group: The carbon company, 2011. [http://www.sglgroup.com]
[43] Wilkie, W. K., Bryant, G. R. and High, J. W., "Low-Cost Piezocomposite Actuator for Structural Control Applications," SPIE 7th Annual International Symposium on Smart Structures and Materials, Newport Beach, CA, 2000.
[44] High, J. W. and Wilkie, W. K., "Method of Fabricating NASA-Standard Macro-Fiber Composite Piezoelectric Actuators," NASA/TM-2003-212427, ARL-TR-2833, 2003.
[45] Hagood, N. W., Kindel, R., Ghandi, K. and Gaudenzi, P., "Improving Transverse Actuation using Interdigitated Surface Electrodes," SPIE Paper No. 1917-25, pp. 341-352, North American Conference on Smart Structures and Materials, Albuquerque, NM, 1993.
[46] Bilgen, O., Erturk, A. and Inman, D.J., "Analytical and Experimental Characterization of Macro-Fiber Composite Actuated Thin Clamped-Free Unimorph Benders," *Journal of Vibration and Acoustics*, Vol. 132, 051005-1, 2010.
[47] Goh, C.J., 1983, "Analysis and Control of Quasi Distributed Parameter Systems," in Department of Mechanical Engineering, California Institute of Technology, Pasadena, CA.
[48] Goh, C.J. and Caughey, T.K., 1985, "On the stability problem caused by finite actuator dynamics in the collocated control of large space structures," *International Journal of Control*, Vol. **41,** pp. 787-802.
[49] Fanson, J.L., and Caughey, T.K., 1990, "Positive position feedback control for large space structures," *AIAA Journal*, Vol. **28**, pp. 717-24.
[50] Dosch, J.J., Calamita, J.P. and Inman, D.J., 1993, "Performance of a programmable structure," Smart Structures and Materials: Mathematics in Smart Structures, Albuquerque, NM.
[51] Friswell, M.I., Inman, D.J., and Rietz, R.W., 1997, "Active damping of thermally induced vibrations," *Journal of Intelligent Material Systems and Structures*," Vol. **8**, pp. 678-85.
[52] Leo, D.J. and Inman, D.J., 1994, "Pointing control and vibration suppression of a slewing flexible frame," *Journal of Guidance, Control, and Dynamics*," Vol. **17**, pp. 529-36.
[53] Tarazaga, P.A., Inman, D.J., and Wilkie, W.K., 2007, "Control of a space rigidizable inflatable boom using macro-fiber composite actuators," *Journal of Vibration and Control*," Vol. **13**, No. 7, pp. 935-950.
[54] Bilgen, O., Wang, Y. and Inman, D. J., 2012, "Electromechanical Comparison of Cantilevered Beams with Multifunctional Piezoceramic Devices," *Mechanical Systems and Signal Processing*, Vol. 27, pp. 763-777. doi:10.1016/j.ymssp.2011.09.002
[55] Crawley, E.F., and Anderson, E.H., 1990, "Detailed Models of Piezoceramic Actuation of Beams," *Journal of Intelligent Material Systems and Structures*, Vol. **1**, pp. 4-25.